Biomech Model Mechanobiol (2013) 12:849–868
DOI 10.1007/s10237-012-0448-x

ORIGINAL PAPER

Development of fibroblast-seeded collagen gels under planar biaxial mechanical constraints: a biomechanical study

Jin-Jia Hu · Yen-Ching Liu · Guan-Wen Chen · Mei-Xuan Wang · Pei-Yuan Lee

Received: 20 July 2012 / Accepted: 9 October 2012 / Published online: 25 October 2012

Abstract Prior studies indicated that mechanical loading influences cell turnover and matrix remodeling in tissues, suggesting that mechanical stimuli can play an active role in engineering artificial tissues. While most tissue culture studies focus on influence of uniaxial loading or constraints, effects of multi-axial loading or constraints on tissue development are far from clear. In this study, we examined the biaxial mechanical properties of fibroblast-seeded collagen gels cultured under four different mechanical constraints for 6 days: free-floating, equibiaxial stretching (with three different stretch ratios), strip-biaxial stretching, and uniaxial stretching. Passive mechanical behavior of the cell-seeded gels was also examined after decellularization. A continuum-based two-dimensional Fung model was used to quantify the mechanical behavior of the gel. Based on the model, the value of stored strain energy and the ratio of stiffness in the stretching directions were calculated at prescribed strains for each gel, and statistical comparisons were made among the gels cultured under the various mechanical constraints. Results showed that gels cultured under the free-floating and equibiaxial stretching conditions exhibited a nearly isotropic mechanical behavior, while gels cultured under the strip-biaxial and uniaxial stretching conditions developed a significant degree of mechanical anisotropy. In particular, gels cultured under the equibiaxial stretching condition with a greater stretch ratio appeared to be stiffer than those with a smaller stretch ratio. Also, a decellularized gel was stiffer than its non-decellularized counterpart. Finally, the retained mechanical anisotropy in gels cultured under the strip-biaxial stretching and uniaxial stretching conditions after cell removal reflected an irreversible matrix remodeling.

Keywords Fibroblast-seeded collagen gels · Tissue development · Mechanical constraints · Mechanical anisotropy · Biaxial mechanical testing · Constitutive modeling

1 Introduction

The extracellular matrix (ECM) provides vital structural integrity for various kinds of tissues. Particularly for load-bearing tissues such as blood vessels, heart valve leaflets, tendons, and ligaments, their load-bearing capacity depends heavily on the organization of the ECM (Kjaer 2004; Wagenseil and Mecham 2009; Lincoln et al. 2006). It is intriguing that most load-bearing tissues develop structural and mechanical anisotropy that reflects their functions. Mechanical conditioning has been used to engineer the load-bearing tissues aiming at better functionality (Seliktar et al. 2000; Mol et al. 2005; Grodzinsky et al. 2000; Mauck et al. 2000; Shearn et al. 2007). In most of these cases, however, the engineered tissue is subjected to a mechanical environment that replicates some aspects of the physiological conditions;

Electronic supplementary material The online version of this article (doi:10.1007/s10237-012-0448-x) contains supplementary material, which is available to authorized users.

J.-J. Hu (✉) · G.-W. Chen · M.-X. Wang · P.-Y. Lee
Department of Biomedical Engineering, National Cheng Kung University, #1 University Rd., Tainan 701, Taiwan
e-mail: jjhu@mail.ncku.edu.tw

J.-J. Hu
Medical Device Innovation Center, National Cheng Kung University, Tainan, Taiwan

Y.-C. Liu
Department of Mechanical Engineering, National Chiao Tung University, Hsinchu, Taiwan

P.-Y. Lee
Department of Orthopedics Surgery, Show Chwan Memorial Hospital, Changhua, Taiwan

it is generally not feasible to correlate the findings (e.g., structural or mechanical anisotropy) in these studies to precise, quantitative mechanical loading or constraints.

Fibroblasts, among the many types of cells within the ECM, play a particularly important role by producing, maintaining, reorganizing, and degrading components of the ECM, in particular collagen. Fibroblast-seeded collagen gels have thus been used as a model system to study cell–matrix interactions in tissue morphogenesis and wound healing (Ehrlich 1988; Bell et al. 1979; Harris et al. 1981). Specifically in tissue engineering, the property of directed collagen contraction in *uniaxially* constrained, rectangular, fibroblast-seeded collagen gels has been used to engineer highly anisotropic load-bearing tissues (Feng et al. 2006; Grenier et al. 2005; Shi and Vesely 2003). Knezevic et al. (2002) were the first to study *biaxially* loaded cell-seeded collagen gels. They developed a novel culture system in which square cell-seeded collagen gels can be subjected to isotonic biaxial loading. Thomopoulos et al. (2005) subsequently used the system to study the development of structural and mechanical anisotropy in the gels and found that gels cultured under a constant uniaxial force developed structural and mechanical anisotropy, whereas gels cultured under constant equibiaxial forces remained mechanically isotropic. Quite a few tissues in the body (e.g., blood vessels, heart valve leaflets, skin, etc.), however, are subjected to neither uniaxial nor equibiaxial loading. Also, to the best of our knowledge, effects of the extent of equibiaxial stretching on tissue development have not been studied. The information is fundamental for increasing our understanding of native tissue mechanics as well as our ability to engineer functional tissue equivalents.

Our novel culture system allowed the application of sophisticated biaxial mechanical constraints (e.g., strip-biaxial stretching) to cruciform-shaped fibroblast-seeded collagen gels (Hu et al. 2009). The previous study, which focused on microstructural changes in fibroblast-seeded collagen gels cultured under defined planar biaxial mechanical constraints, demonstrated that the microstructure of the fibroblast-seeded collagen gels can be manipulated by the biaxial mechanical constraints (Hu et al. 2009). It is unclear, however, how well the microstructural findings can be correlated to mechanical properties. As the functionality of load-bearing tissues is more related to their mechanical properties, in this study we examined the biaxial mechanical properties of cruciform-shaped fibroblast-seeded collagen gels cultured under various mechanical constraints. We used tension-controlled protocols to examine the biaxial mechanical properties of the gels. Passive mechanical properties of the gels, which were determined after decellularization, were also examined. Finally, a continuum-based two-dimensional (2-D) Fung model was used to quantify the mechanical behavior of the decellularized gels, allowing calculation of the value of stored strain energy as well as the ratio of stiffness in the stretching directions of the gels. Specifically, for evaluation of the predictive capability of the model, the model with material parameters determined by fitting proportional tension data of a decellularized gel was used to simulate the mechanical behavior of the gel under equibiaxial tension.

2 Methods

2.1 Preparation of cruciform-shaped fibroblast-seeded collagen gels

3T3 fibroblasts were cultured in DMEM containing 10 % calf serum and antibiotics and passaged for every 6–7 days. Confluent cells were detached by 0.05 % trypsin-EDTA, counted, and resuspended in culture medium at 2.3×10^6 cells/mL to be incorporated into collagen gels. Cell-seeded collagen gels were prepared on ice to avoid premature gelation. Specifically, 0.45 mL of reconstituted buffer (10×) was mixed with 0.9 mL of DMEM solution (5×) and 1.2 mL of concentrated collagen type I (9.37 mg/mL; BD Biosciences, San Jose, CA), mixed thoroughly, and then neutralized by ∼110 mL of 0.1 N sodium hydroxide before adding 1.95 mL of the cell suspension (or DMEM solution (1×) for acellular gels). The final densities of cell and collagen were 1×10^6 cells/mL and 2.68 mg/mL, respectively. This mixture was poured into a cruciform mold (Fig. 1a) consisting of a silicone gasket

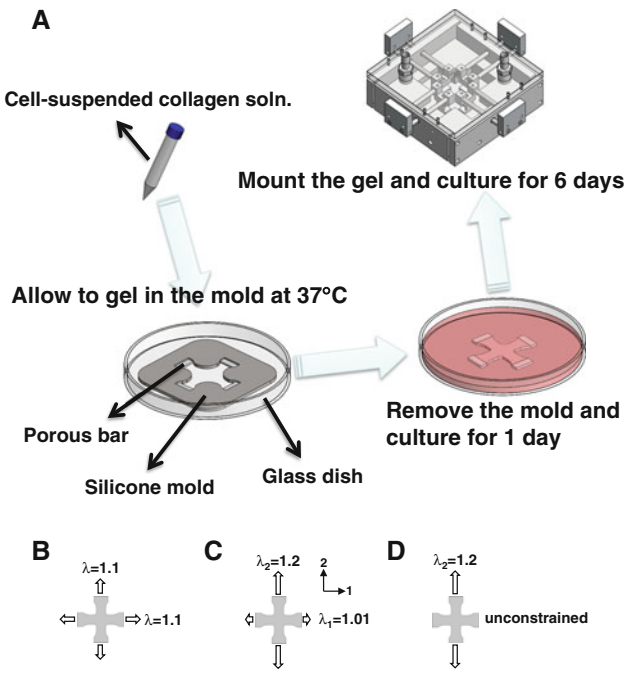

Fig. 1 Schematic diagram showing how a cruciform-shaped fibroblast-seeded collagen gel is made and clamped to the biaxial tissue culture chamber (**a**). The cell-seeded gels are constrained equibiaxially (**b**), strip-biaxially (**c**), or uniaxially (**d**) in the chamber

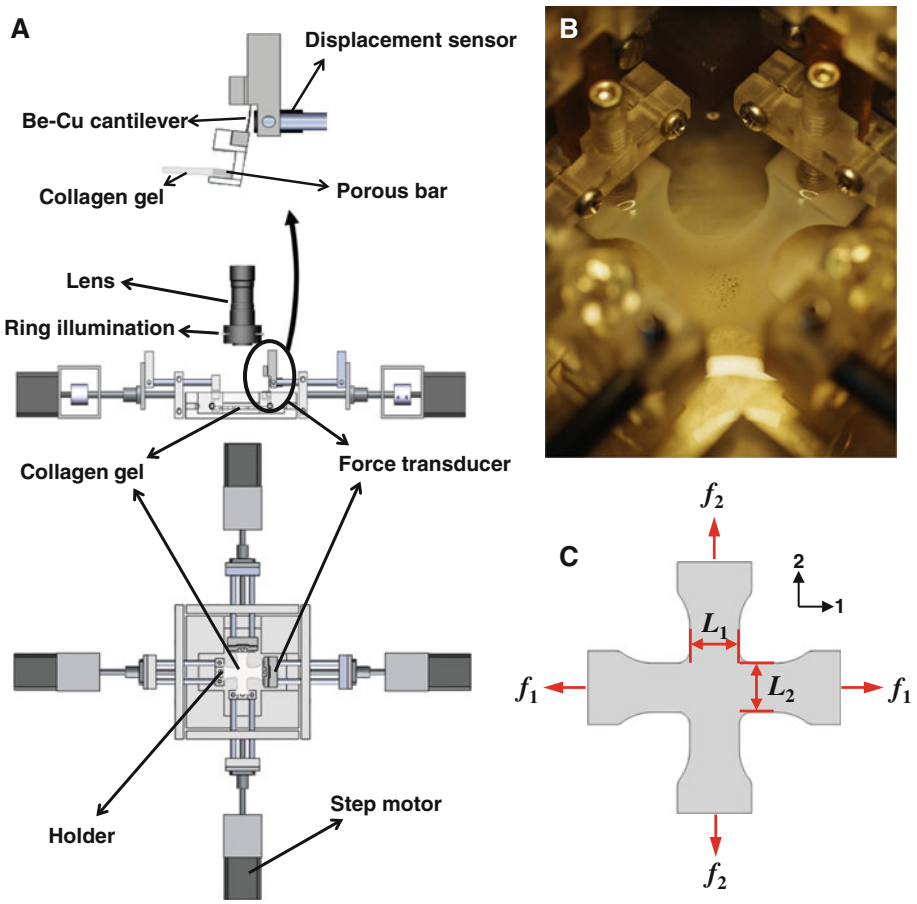

Fig. 2 (**a**) *Top view* and *side view* of the custom-made planar biaxial mechanical tester with detailed illustration of the custom-made force transducer. (**b**) A photograph showing a decellularized gel clamped to the force transducers and holders with tracking markers on its surface. (**c**) Schematic drawing showing the axial forces and the undeformed transverse lengths that are used to determine the first Piola–Kirchhoff tensions

placed within a 150 × 20 (diameter×height, mm) glass Petri dish. Porous polyethylene bars (Small Parts, Miramar, FL) were positioned at each end of the four arms of the mold before adding the collagen–cell mixture. Cell-seeded collagen gels were formed in the mold at 37 °C in a humidified CO_2 incubator. The silicone gasket was removed after 30 min of gelation, and the collagen gel was cultured in 40 mL of culture media within an incubator for an additional 24 h before subjecting to a specific mechanical constraint.

2.2 Biaxial tissue culture chamber and culturing conditions

Cell-seeded collagen gels were cultured under four different static mechanical constraints: free-floating, equibiaxial stretching (λ_1:λ_2 = 1.01:1.01, 1.1:1.1, and 1.2:1.2, where λ_1 and λ_2 are the global stretch ratios in the 1 and 2 directions, respectively), strip-biaxial stretching (λ_1:λ_2 = 1.01:1.2), and uniaxial stretching (λ_2 = 1.2) (Fig. 1b). For the free-floating condition, cruciform-shaped cell-seeded collagen gels were simply cultured in a Petri dish at 37 °C in a humidified CO_2 incubator for 6 days. For all the other conditions, a custom biaxial tissue culture chamber was used to impart the defined planar biaxial mechanical constraints to the cell-seeded collagen gel (Humphrey et al. 2008). Briefly, the chamber was sterilized with autoclave before use. Under aseptic conditions, the cell-seeded collagen gel was clamped within the chamber via the porous polyethylene bars embedded at the end of its arms and stretched uniaxially or biaxially. The chamber was then covered and placed in a 37 °C humidified CO_2 incubator for 6 days.

2.3 Planar biaxial mechanical testing

A modified version of the biaxial test system described by Wells et al. (2006) was employed. Briefly, the system consists of four loading assemblies, a CCD camera with a zoom lens, two custom-made, highly sensitive force transducers, a specimen chamber, and a PC (Fig. 2). The four loading assemblies are driven by PC-controlled step motors to cyclically stretch the cruciform-shaped gel along its arms. The deformation within the central region of the gel is monitored by the CCD camera, and the tensile force in each axis is measured by the force transducer. Specifically, the force transducer is composed of a cantilever beam (Be–Cu alloy) to which a gripper is attached, and a displacement sensor (EX-110V, Keyence, Japan) for measuring the deflection of the cantilever. The stiffness of the Be–Cu alloy as well as the dimensions of the cantilever was selected to minimize the deflection of

the cantilever at the target sensing range (0–5 mN). The force transducer was calibrated with known weights within the sensing range; the relationship between the weight and the deflection appeared to be linear within the range. The motion control, vision, and data acquisition of the system are integrated by LabVIEW (National Instruments, Austin, TX). In this study tension-controlled protocols were used, in which the ratio of the axial first Piola–Kirchhoff tensions (i.e., T_{11}:T_{22}) was kept constant by two independent virtual PID controllers (one for each axis) during the loading and unloading cycle. The first Piola–Kirchhoff tensions are defined as $T_{11}^{\text{Exp}} = f_1/L_2$ and $T_{22}^{\text{Exp}} = f_2/L_1$ where f_1 and f_2 are the measured tensile forces in the 1 and 2 directions, respectively, and L_1 and L_2 are the undeformed transverse length in the 1 and 2 directions, respectively (Fig. 2c). Our preliminary experiments showed that the mechanical response of the gel was dependent on the strain rate (see Supplemental Figure 1 for an example). Thus, quasi-static loading was used in the test. Note that tension (also called stress resultant or membrane stress), instead of stress, was used to characterize the mechanical behavior of the gel for at least two reasons. First, the gel is thin with negligible bending stiffness; it can thus be approximated as a membrane. Second, as the gel is highly hydrated, it is difficult to measure its thickness reproducibly; the accuracy of the calculated stress is compromised. Note, furthermore, that most water in the gel is not confined, and the total volume of the gel may change during the test. The incompressibility may not be used to determine the out-of-plane strain; it is thus not possible to derive the three-dimensional constitutive model of the gel from our planar biaxial data.

After 6 days of culture, the chamber with the gel was removed from the incubator and mounted onto the biaxial test system. One holder in each axis was replaced by the force transducer. A number of 50-micron markers were delivered onto the surface of a central region of the gel and allowed to affix to the gel; at least nine of these markers were video-tracked to determine the 2-D deformation gradient tensor $\mathbf{F}_{2D}$ of the region throughout the test (see Hu et al. (2007) for details). The gel was preconditioned equibiaxially for 3–5 times, and then the unloaded reference configuration was recorded. Subsequently, the gel was tested using an equibiaxial tension protocol (T_{11}:T_{22} = 1:1). After the mechanical contribution of cell traction was removed via osmotic shock, the decellularized gel was subjected to the same testing procedures for measuring its passive mechanical properties. In addition, proportional tension protocols (T_{11}:T_{22} = 0.5:1, 0.75:1, 1:0.75, 1:0.5) were performed on the decellularized gel. Note that the equibiaxial tension protocol was performed after the equibiaxial preconditioning and repeated following the proportional tension protocols. The results of the two equibiaxial tension tests were compared to ensure that no mechanical damage occurred. For all of the gels tested in this study, the results of the two tests were similar, indicating the loadings were within the elastic range of the gels. Note also that the kinematic analysis for a non-decellularized gel and its decellularized counterpart was based on distinct, unloaded reference configurations.

In this study the first Piola–Kirchhoff tension and the stretch ratio were used to characterize the mechanical behavior of the gel. Note that the first Piola–Kirchhoff tension is conjugate to the deformation gradient and hence to the stretch ratio in this case. The stretch ratios in the 1 and 2 directions are extracted from the deformation gradient assuming that in-plane shears are negligible. That is, $\lambda_1 = F_{11}$ and $\lambda_2 = F_{22}$. As an important strain measure for modeling mechanical behavior, the 2-D Green strain tensor was also calculated using $\mathbf{E}_{2D} = \frac{1}{2}\left(\mathbf{F}_{2D}^T \cdot \mathbf{F}_{2D} - \mathbf{I}\right)$. In addition, the rigid body rotation angle ϕ was determined using $\phi = \tan^{-1}\left(\frac{F_{12}-F_{21}}{F_{11}+F_{22}}\right)$ (Mcculloch et al. 1987). Based on the tension-stretch data, mechanical anisotropy of the gel was quantified by an anisotropy index, defined as the ratio of the difference in stretch $|\lambda_2 - \lambda_1|$ to the mean stretch $(\lambda_1 + \lambda_2)/2$ under 0.1 N/m *equibiaxial* tension (Langdon et al. 1999). Note that the anisotropy index is not valid as a measure of anisotropy for proportional tension protocols. A perfectly isotropic gel has an anisotropy index of zero. The greater the anisotropy index, the stronger the mechanical anisotropy of the gel.

2.4 Constitutive modeling

The nonlinear, anisotropic pseudo-elastic mechanical behavior of cell-seeded collagen gels was quantified by a hyperelastic model. Consider a general nonlinear, anisotropic membrane subjected to an in-plane biaxial stretching wherein the deformation gradient is, in matrix form, as follows:

$$[\mathbf{F}] = \begin{bmatrix} F_{11} & F_{12} & 0 \\ F_{21} & F_{22} & 0 \\ 0 & 0 & \lambda_3\,(=h/H) \end{bmatrix}$$

where h and H are the thickness of the membrane in its deformed and undeformed configurations, respectively. A general 2-D constitutive relation between the 2-D Cauchy stress $\boldsymbol{\sigma}_{2D}$ and strain energy w, defined per unit undeformed area, can be derived as follows (Humphrey et al. 1992):

$$\boldsymbol{\sigma}_{2D} = \frac{1}{hJ_{2D}}\mathbf{F}_{2D} \cdot \frac{\partial w}{\partial \mathbf{E}_{2D}} \cdot \mathbf{F}_{2D}^T$$

where $J_{2D} = F_{11}F_{22} - F_{12}F_{21}$ is the determinant of $\mathbf{F}_{2D}$. The 2-D first Piola–Kirchhoff stress tensor is determined using $\mathbf{P}_{2D} = \frac{1}{H}\frac{\partial w}{\partial \mathbf{E}_{2D}} \cdot \mathbf{F}_{2D}^T$. The in-plane first Piola–Kirchhoff tension tensor is then as follows:

$$\mathbf{T} = H\mathbf{P}_{2D} = \frac{\partial w}{\partial \mathbf{E}_{2D}} \cdot \mathbf{F}_{2D}^T.$$

Table 1 The maximum shear strain and maximum rigid body rotation angle in the central region of acellular gels and cell-seeded gels cultured under the various mechanical constraints throughout the test

	Acellular ($N = 6$)	Free floating ($N = 5$)	1.01×1.01 ($N = 6$)	1.1×1.1 ($N = 5$)	1.2×1.2 ($N = 5$)	1.01×1.2 ($N = 5$)	Uniaxial_1.2 ($N = 5$)
Non-decellularized							
Max$\lvert E_{12}\rvert$	–	0.02 ± 0.00	0.02 ± 0.01	0.02 ± 0.02	0.00 ± 0.00	0.01 ± 0.01	0.01 ± 0.01
Max$\lvert\phi\rvert$	–	0.57 ± 0.24	0.48 ± 0.27	0.49 ± 0.41	0.23 ± 0.08	0.27 ± 0.24	0.33 ± 0.31
Decellularized							
Max$\lvert E_{12}\rvert$	0.01 ± 0.01	0.00 ± 0.00	0.00 ± 0.01	0.00 ± 0.00	0.01 ± 0.01	0.00 ± 0.00	0.00 ± 0.00
Max$\lvert\phi\rvert$	0.33 ± 0.23	0.23 ± 0.10	0.27 ± 0.20	0.25 ± 0.19	0.24 ± 0.22	0.15 ± 0.09	0.12 ± 0.06

The angles are displayed in degrees. Results are presented as mean ± standard deviation

To fit the biaxial tension-strain data of the gel before or after decellularization, we used a 2-D Fung-type exponential strain energy function w of the form:

$$w = \frac{c}{2}\left(\exp^{Q} - 1\right)$$

where $Q = c_1 E_{11}^2 + c_2 E_{22}^2 + 2c_3 E_{11} E_{22}$ and c, c_1, c_2 and c_3 are material parameters, and E_{11} and E_{22} are components of the 2-D Green strain tensor in the 1 and 2 directions, respectively. Note, to satisfy physical and mathematical (convexity) constraints, $c > 0, c_1 > 0, c_2 > 0, c_3 > 0$ and $c_1 c_2 > c_3^2$ (Humphrey 1999; Holzapfel et al. 2000). The nonzero components of $\mathbf{T}$ are as follows:

$$T_{11}^{\text{Theory}} = cF_{11}\exp^{Q}\left(c_1 E_{11} + c_3 E_{22}\right), \quad \text{and}$$
$$T_{22}^{\text{Theory}} = cF_{22}\exp^{Q}\left(c_2 E_{22} + c_3 E_{11}\right).$$

Best-fit material parameters for each gel were determined using a nonlinear regression. This was accomplished using a modified fminsearch function (Matlab) to minimize the objective function (fitting error):

$$e = \sum_{i=1}^{N}\left[\left(T_{11}^{\text{Theory}} - T_{11}^{\text{Exp}}\right)_i^2 + \left(T_{22}^{\text{Theory}} - T_{22}^{\text{Exp}}\right)_i^2\right].$$

The goodness of fit for the model was assessed by the coefficient of determination (r^2).

Given the material parameters, the value of stored strain energy of the gel, which was used as a stiffness index, was calculated at $E_{11} = E_{22} = 0.05$. The higher the stored strain energy, the stiffer the gel. The material stiffness tensor of the gel, defined as $\mathbf{K} = \frac{\partial \mathbf{S}_{2D}}{\partial \mathbf{E}_{2D}}$ where $\mathbf{S}_{2D} = \frac{\partial w}{\partial \mathbf{E}_{2D}}$ is the 2-D second Piola–Kirchhoff tension tensor, was also determined. Particularly, the ratio of stiffness in the 1 and 2 directions (i.e., $(K)_{1111}/K_{2222}$) was calculated at $E_{11} = E_{22} = 0.05$ and used as another anisotropy index. Note that the second Piola–Kirchhoff tension is conjugate to the Green strain.

Finally, for evaluation of the predictive capability of the model, results of proportional tension protocols (excluding the equibiaxial tension protocol) from a decellularized gel were fit for the material parameters. The material parameters were then used to simulate the mechanical behavior of the gel under equibiaxial tension.

2.5 Statistical analysis

Differences before and after decellularization were assessed via paired t test. For comparisons among the various mechanical constraints, one-way ANOVA with Holm–Sidak post hoc testing (significance level $p = 0.05$) was used. Holm–Sidak testing is useful to correct for false positives enumerated by the Bonferroni inequality and adequate for the relatively few number of comparisons in this study. Results are reported as mean ± standard deviation.

3 Results

3.1 Validation of the biaxial mechanical testing

For all of the acellular gels and cell-seeded gels examined in this study, the shear strain (E_{12}) and the rigid body rotation angle (ϕ) in the central region were negligible throughout the test (Table 1 and Supplemental Figure 2).

3.2 Biaxial mechanical properties of the cell-seeded collagen gels

The anisotropy indices of the gels, determined based on the tension-stretch data, are shown in Fig. 3. Although gels cultured under the free-floating condition had a greater variation in anisotropy index than those subjected to the equibiaxial stretching conditions, the anisotropy indices of all of these gels as well as acellular gels were close to zero. On the other hand, gels cultured under the strip-biaxial stretching condition had a moderate anisotropy index, while gels cultured under the uniaxial stretching condition had a higher anisotropy index. Moreover, the anisotropy indices of the gels did not change significantly after decellularization for all of the

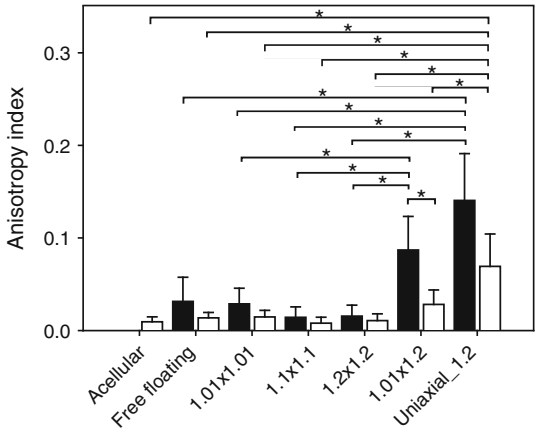

Fig. 3 Anisotropy indices of acellular gels and cell-seeded gels cultured under the various mechanical constraints. *Solid bars* represent non-decellularized gels, while *open bars* represent acellular and decellularized gels. *Asterisk* means $p < 0.05$

mechanical constraints except the 1.01×1.2 strip-biaxial stretching condition.

As acellular gels and cell-seeded gels cultured under the free-floating and equibiaxial stretching conditions appeared to be isotropic, it seems reasonable to combine tension-stretch data of the two orthogonal axes for analysis; it is in fact not practical to define the 1 and 2 directions in these cases as the mechanical constraints in both directions are no different. Figure 4 shows that for cell-seeded gels cultured under the equibiaxial stretching conditions, the gels became stiffer as the stretch ratio increased. Moreover, compared with the acellular gels, all of the cell-seeded gels appeared to be less stiff. Also, a decellularized gel was stiffer than its non-decellularized counterpart. Note that the stretches were calculated based on different unloaded reference configurations for a non-decellularized gel and its decellularized counterpart. Again, gels cultured under the free-floating condition exhibited a great variation in the tension-stretch curves. After decellularization, the tension-stretch curves of the gels appeared to be more linear. Although the decellularized gels appeared stiffer in the case of the 1.2×1.2 equibiaxial stretching condition, the difference in tension-stretch curves among the five groups was not significant.

Figure 5 shows that gels cultured under the strip-biaxial stretching condition developed a moderate degree of mechanical anisotropy while gels cultured under the uniaxial stretching condition developed a strong degree of mechanical anisotropy. Both groups of the gels became stiffer after decellularization. The mechanical anisotropy after decellularization appeared to be preserved well in the case of the uniaxial stretching condition and less well in the case of the strip-biaxial stretching condition.

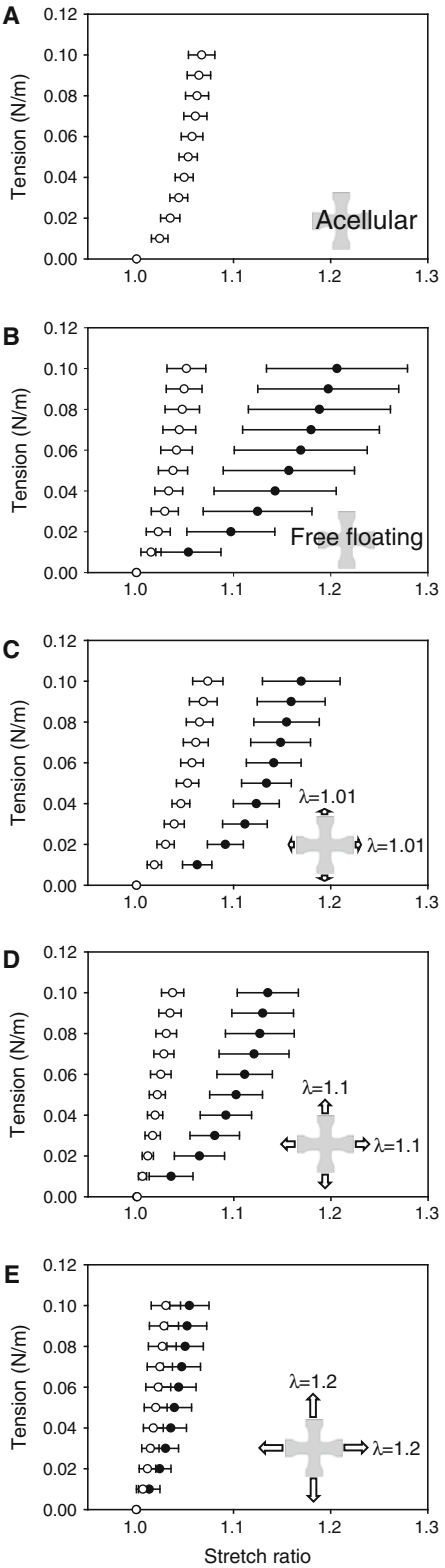

Fig. 4 Equibiaxial tension data for acellular gels (**a**) and cell-seeded gels cultured under free-floating (**b**) and equibiaxial stretching (**c** 1.01×1.01, **d** 1.1×1.1, **e** 1.2×1.2) conditions. *Solid symbols* represent non-decellularized gels, while *open symbols* represent decellularized gels

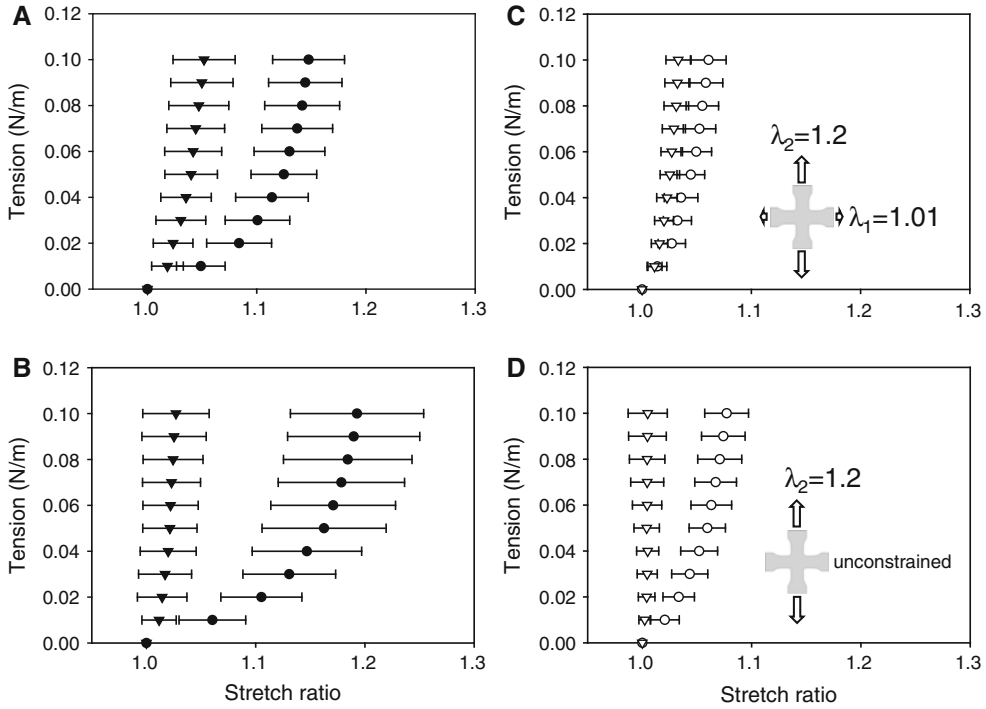

Fig. 5 Equibiaxial tension data for cell-seeded gels cultured under strip-biaxial stretching (**a** and **c** 1.01 × 1.2) and uniaxial stretching (**b** and **d** unconstrained × 1.2) conditions. *Solid symbols* represent non-decellularized gels (**a** and **b**), while *open symbols* represent decellularized gels (**c** and **d**). *Filled circle and open circle* $T_{11} - E_{11}$, *filled inverted triangle and open inverted triangle* $T_{22} - E_{22}$

3.3 Constitutive modeling

The Fung model was used to quantify the mechanical characteristics of the gels. Best-fit values of the material parameters obtained by fitting the Fung model to equibiaxial tension data of each cell-seeded gel and its decellularized counterpart are listed in Tables 2 and 3, respectively. The Fung model provided great fitting to the equibiaxial tension data, and the coefficient of determination (r^2) for each fitting was greater than 0.98. Nevertheless, if the data of each gel in the same group were combined and fitted for the Fung model, the r^2 for each fitting was significantly worse.

The value of stored strain energy for each gel was calculated based on the material parameters in Tables 2 and 3. Figure 6 shows the statistical comparisons of the values of stored strain energy for acellular gels and cell-seeded gels cultured under the free-floating and equibiaxial stretching conditions. There was significant difference between the 1.2 × 1.2 equibiaxial stretching and other groups before decellularization. After decellularization, gels cultured under the 1.2 × 1.2 equibiaxial stretching and 1.01 × 1.01 equibiaxial stretching conditions remained significantly different. Furthermore, gels cultured under the 1.2 × 1.2 equibiaxial stretching condition stored significantly greater strain energy than acellular gels at the prescribed strains. Note that all of the groups showed significant difference in the value of stored strain energy before and after decellularization except the 1.2 × 1.2 equibiaxial stretching condition.

Also calculated based on the modeling results, the ratio of stiffness in the stretching directions was served as another index for mechanical anisotropy. The comparisons of the ratios of stiffness among the seven groups are shown in Fig. 7. Consistent with the findings in Fig. 3, the ratios of stiffness were close to one for gels cultured under free-floating and equibiaxial stretching conditions, while those for gels cultured under the strip-biaxial stretching and uniaxial stretching conditions were less than one. There was significant difference between the uniaxial stretching and other groups before decellularization except the pair of the uniaxial and strip-biaxial stretching conditions. After decellularization, significant differences were observed between the uniaxial stretching and all of the other groups. No significant difference in the ratio of stiffness was found before and after decellularization for each group, however.

Best-fit values of the material parameters obtained by fitting the Fung model to proportional tension data of each acellular gel and decellularized gel are listed in Table 4. Fair fittings of the proportional tension data were achieved for the Fung model, and the mean r^2 for each group was ranged from 0.88 to 0.99. Again, if the data of each gel in the same group were combined and fitted for the Fung model, the r^2 for each fitting was significantly worse.

Table 2 Best-fit values of the material parameters and the goodness of fit for the Fung model for each cell-seeded gel cultured under the various mechanical constraints (non-decellularized gels)

Specimen	Material parameters				Goodness of fit
	c (mN/m)	c_1	c_2	c_3	r^2
Free floating					
1	152.94	0.81	0.75	0.78	0.999
2	7.00	12.97	12.49	11.71	0.996
3	45.19	2.59	3.62	3.06	0.995
4	7.24	4.15	4.10	4.12	0.998
5	14.18	7.58	9.22	8.36	0.996
Group	170,161.61	0.00	0.00	0.00	0.753
1.01 × 1.01					
1	3.70	14.36	12.98	12.95	0.999
2	3.85	21.02	21.07	21.04	0.997
3	30.60	5.57	5.01	0.81	0.998
4	4.41	18.63	16.88	17.73	0.999
5	16.00	5.05	5.36	5.20	0.997
6	5.63	9.45	9.88	8.43	0.998
Group	32.87	0.52	0.52	0.52	0.829
1.1 × 1.1					
1	10.77	11.39	12.26	11.06	0.998
2	28.59	5.72	5.51	5.43	0.999
3	13.84	5.72	5.66	5.69	0.995
4	17.35	15.04	14.39	10.40	0.997
5	7.89	21.72	20.36	16.70	0.999
Group	99,680.24	0.00	0.00	0.00	0.784
1.2 × 1.2					
1	4.65	75.23	69.30	16.92	0.996
2	11.85	59.89	61.72	60.80	0.993
3	13.11	74.48	73.69	74.09	0.988
4	4.99	73.23	72.50	72.86	0.999
5	8.33	33.61	35.03	34.31	0.999
Group	83.13	9.77	0.68	0.72	0.790
1.01 × 1.2					
1	2.01	13.86	13.21	13.53	0.994
2	15.13	19.94	22.51	21.18	0.993
3	10.20	13.99	13.89	13.94	0.990
4	5.97	20.08	24.71	22.28	0.999
5	5.02	38.61	48.42	43.24	0.999
Group	59,011.98	0.00	0.00	0.00	0.779
Uniaxial_1.2					
1	5.56	10.37	43.42	10.93	0.999
2	4.70	24.22	48.87	17.89	0.999
3	2.36	30.78	73.18	23.16	0.999
4	10.04	28.84	38.48	33.31	0.991
5	11.59	29.08	36.08	32.39	0.986
Group	160,841.13	0.00	0.00	0.00	0.673

Table 3 Best-fit values of the material parameters and the goodness of fit for the Fung model for each acellular gel and cell-seeded gel cultured under the various mechanical constraints (decellularized gels)

Specimen	Material parameters				Goodness of fit
	c (mN/m)	c_1	c_2	c_3	r^2
Acellular					
1	2.22	121.81	122.90	121.57	0.999
2	3.27	84.71	81.10	65.71	0.999
3	1.34	77.92	75.03	71.22	0.999
4	3.70	48.81	49.78	49.29	0.994
5	0.87	122.09	123.57	122.83	0.993
6	11.13	23.43	24.01	23.72	0.998
Group	63.38	0.79	0.78	0.79	0.843
Free floating					
1	44.16	11.20	10.82	11.01	0.996
2	5.48	148.48	159.84	113.30	0.999
3	7.45	72.86	68.59	67.36	0.999
4	2.17	72.82	72.42	72.62	0.998
5	14.28	69.86	69.28	69.57	0.997
Group	88.17	0.80	0.71	0.75	0.728
1.01 × 1.01					
1	5.66	37.71	36.97	37.34	0.999
2	3.39	113.49	109.49	107.21	0.999
3	578.12	0.91	0.93	0.92	0.994
4	6.88	48.07	43.59	36.13	0.999
5	10.21	24.38	25.96	25.16	0.999
6	5.96	37.47	37.20	37.33	0.999
Group	64.57	0.76	0.80	0.78	0.885
1.1 × 1.1					
1	2,342.75	0.81	0.80	0.80	0.982
2	377,132.85	0.00	0.00	0.00	0.997
3	30.90	43.03	43.99	43.29	0.999
4	16.63	45.12	45.49	45.30	0.988
5	9.54	61.31	57.28	46.63	0.998
Group	140.34	0.80	0.73	0.76	0.818
1.2 × 1.2					
1	13.30	155.31	145.13	121.02	0.997
2	4.70	113.66	114.05	113.85	0.983
3	14.57	242.55	259.84	1.03	0.996
4	142.15	9.62	9.41	9.52	0.993
5	5.70	79.61	81.67	80.63	0.999
Group	132.72	0.85	0.70	0.77	0.70
1.01 × 1.2					
1	5.66	59.23	80.76	50.66	0.999
2	5.64	128.50	136.47	132.43	0.999
3	4.20	86.07	87.69	86.87	0.999
4	4.24	97.43	110.42	97.71	0.999
5	7.79	105.94	112.02	108.94	0.990
Group	104.92	0.76	0.80	0.78	0.825

Table 3 Continued

Specimen	Material parameters				Goodness of fit
	c (mN/m)	c_1	c_2	c_3	r^2
Uniaxial_1.2					
1	8.51	80.73	116.53	73.74	0.999
2	4.53	117.73	127.35	122.44	0.998
3	2.70	119.09	199.01	110.52	0.999
4	3.87	94.89	109.44	101.91	0.993
5	2.61	191.05	313.60	222.10	0.999
Group	100.67	0.84	1.00	0.91	0.897

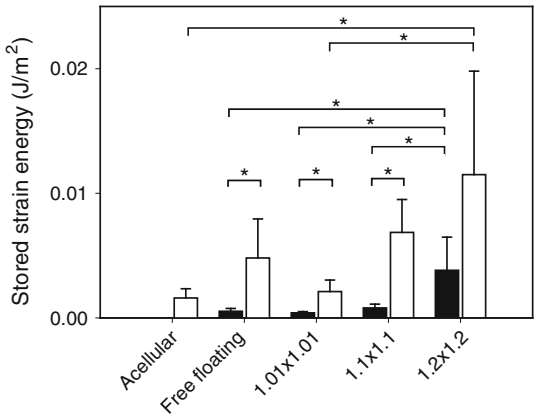

Fig. 6 Values of stored strain energy of acellular gels and cell-seeded gels cultured under free-floating and equibiaxial stretching conditions. *Solid bars* represent non-decellularized gels, while *open bars* represent acellular and decellularized gels. *Asterisk* means $p < 0.05$

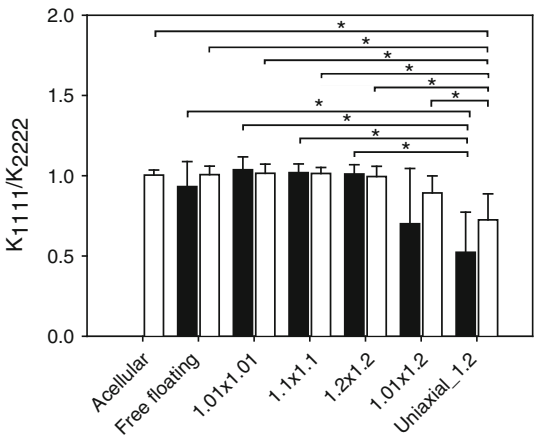

Fig. 7 Ratios of stiffness in the stretching directions of acellular gels and cell-seeded gels cultured under the various mechanical constraints. *Solid bars* represent non-decellularized gels, while *open bars* represent acellular and decellularized gels. *Asterisk* means $p < 0.05$

Figures 8, 9, 10, 11, 12, 13, 14 show the proportional tension data of acellular gels and decellularized gels that were cultured under the various mechanical constraints and their fits by the Fung model. The Fung model appeared to fit

Table 4 Best-fit values of the material parameters and the goodness of fit for the Fung model for each acellular gel or cell-seeded gel cultured under the various mechanical constraints (Decellularized gels)

Specimen	Material parameters				Goodness of fit
	c (mN/m)	c_1	c_2	c_3	r^2
Acellular					
1	2.10	189.13	161.99	85.02	0.982
2	3.02	86.81	111.34	38.32	0.909
3	2.17	80.04	84.50	31.94	0.929
4	375.77	2.47	1.95	0.99	0.853
5	339,872.30	0.00	0.00	0.00	0.798
6	29.71	33.58	27.38	11.51	0.874
Group	17,459.75	0.00	0.00	0.00	0.828
Free floating					
1	21.68	32.06	28.02	10.88	0.997
2	3.32	278.78	371.18	92.29	0.986
3	513,065.07	0.00	0.00	0.00	0.759
4	2.83	88.96	236.45	57.70	0.948
5	14.01	78.03	133.65	68.22	0.984
Group	67,837.15	0.00	0.00	0.00	0.701
1.01 × 1.01					
1	8.75	58.53	49.41	23.20	0.984
2	3.66	218.06	156.85	92.19	0.993
3	452,563.69	0.00	0.00	0.00	0.995
4	3.71	104.00	83.83	43.53	0.985
5	6.91	43.16	61.14	16.46	0.994
6	5.78	71.18	76.10	19.76	0.989
Group	6,472.02	0.01	0.01	0.01	0.864
1.1 × 1.1					
1	50.90	85.03	119.82	69.21	0.970
2	280.43	5.80	6.21	2.77	0.988
3	23.64	59.24	86.13	41.71	0.957
4	304.56	8.72	8.98	4.47	0.969
5	61.37	20.73	21.27	7.86	0.921
Group	30,449.79	0.01	0.01	0.00	0.758
1.2 × 1.2					
1	349,332.41	0.01	0.01	0.00	0.887
2	720,146.66	0.00	0.00	0.00	0.684
3	30,907.94	0.37	0.37	0.30	0.956
4	23.17	79.35	90.22	47.08	0.941
5	110,067.69	0.02	0.02	0.01	0.939
Group	32,673.88	0.01	0.00	0.00	0.682
1.01 × 1.02					
1	3.68	85.91	170.93	50.99	0.991
2	3.14	210.19	307.08	95.22	0.974
3	3.91	117.90	153.26	43.31	0.984
4	4.03	138.10	190.75	86.42	0.967
5	2.18	241.48	508.55	182.95	0.992
Group	8,718.09	0.01	0.01	0.01	0.828

Table 4 Continued

Specimen	Material parameters				Goodness of fit
	c (mN/m)	c_1	c_2	c_3	r^2
Unload_1.02					
1	3.94	131.15	353.94	78.64	0.989
2	4.15	126.46	327.47	78.47	0.983
3	2.55	118.55	303.23	77.41	0.990
4	3.00	124.48	205.27	121.84	0.903
5	4.73	140.84	295.85	157.10	0.931
Group	0.62	23.54	39.19	21.61	0.836

the nonlinear mechanical behavior of the gels well, particularly the gels cultured under strip-biaxial stretching and uniaxial stretching conditions. Inconsistent fittings of proportional tension data were observed, however, if the mechanical behavior of the gels appeared to be linear and isotropic. Note that if an exceptional large c was obtained, the fitting came along with negligible c_1, c_2, and c_3.

3.4 Predictive capability of the constitutive model

The material parameters for each gel in Table 4 were used to simulate the mechanical behavior of the gel under equibiaxial tension. Figure 15 illustrates the experimental and simulated equibiaxial tension data of a representative acellular gel and representative decellularized gels that were cultured under the various mechanical constraints. It appeared that the predictive capability of the Fung model for the gels was fair.

4 Discussion

The microstructure of the cell-seeded collagen gels developed under the various mechanical constraints was investigated previously (Hu et al. 2009). Changes in mechanical properties due to the mechanical constraints were identified in this study. Similar to the microstructural findings, the biaxial mechanical properties of the gels appeared to be influenced by the mechanical constraints. Notably, the mechanical isotropy or anisotropy observed in this study appeared to be correlated well with the irreversible collagen fiber alignment shown in the previous study (Hu et al. 2009).

Specifically in this study, we quantified and compared, for the first time, the biaxial mechanical properties of the cell-seeded collagen gels cultured under different extents of equibiaxial stretching. Contrary to previous findings that cell-seeded gels become stiffer when they are allowed to contract (Chen et al. 2008; Berry et al. 2009), cell-seeded gels cultured under the 1.2 × 1.2 equibiaxial stretching condition displaced the stiffest mechanical properties among the other equibiaxial stretching conditions as well as the free-floating condition, particularly before the gels were decellularized. Uniaxially constrained, rectangular cell-seeded collagen gels tend to contract laterally over time in culture, resulting in an axially stiffer gel (Feng et al. 2006; Grenier et al. 2005; Shi and Vesely 2003). We further showed that applied uniaxial stretch expedited and enhanced the structural remodeling if the gel was laterally unconstrained (Hu et al. 2009). The stiffness increase in the uniaxially constrained gels is mainly due to the enhanced fiber alignment, which, however, may not be responsible for the stiffness increase in the equibiaxially constrained gels as their microstructure remained isotropic. The stiffness increase in gels cultured under the 1.2 × 1.2 equibiaxial stretching condition may be in part attributed to a mechanism underlying the so-called plastic compression. Plastic compression is essentially an irreversible process of water expulsion accomplished by unconfined compression of the collagen gel (Brown et al. 2005). The collagen gel is a random mesh of collagen fibers embedded in a significant amount of fluid (99 %). The excess fluid in the gel is a result of the casting, rather than any inherent swelling property of the collagen (Brown et al. 2005). This unique property may allow the applied equibiaxial stretching to enhance the mechanical properties of the collagen gel without the participation of cells. Note, however, that in preliminary experiments biaxial mechanical properties of the gel were examined before and after enforcing the various mechanical constraints to ensure that the extent of each mechanical constraint did not cause irreversible mechanical changes. Therefore, all of the mechanical changes in the gels after 6 days of culture might be well attributed to a cell-mediated matrix remodeling process. Although the 1.2 × 1.2 equibiaxial stretching is still within the elastic range of the gels, the applied equibiaxial stretching might enhance the cell-mediated gel contraction, facilitating irreversible water expulsion and resulting in a stiffer gel. It is interesting to note that Thomopoulos et al. (2005) reported that acellular gels also yielded irreversible mechanical anisotropy when subjected to a constant uniaxial force (200 mg); that is, the presence of cells is not responsible for the change. In that case the applied uniaxial force may exceed the elastic limit of the gel and cause plastic deformation. Nevertheless, our preliminary experiments showed that acellular gels cultured under the uniaxial stretching condition did not develop mechanical anisotropy over time, implicating the importance of cell-mediated matrix remodeling. Note also that gels were cultured under isotonic mechanical loadings in their studies, whereas gels were cultured under isometric mechanical constraints in our studies.

In the biaxial mechanical testing of the gels, the resistance due to interstitial fluid flow is negligible compared to that for stretching the solid network phase (Chandran and Barocas 2004). Also, quasi-static loading that was used during the test minimized the viscous effect of the gel on its mechanical

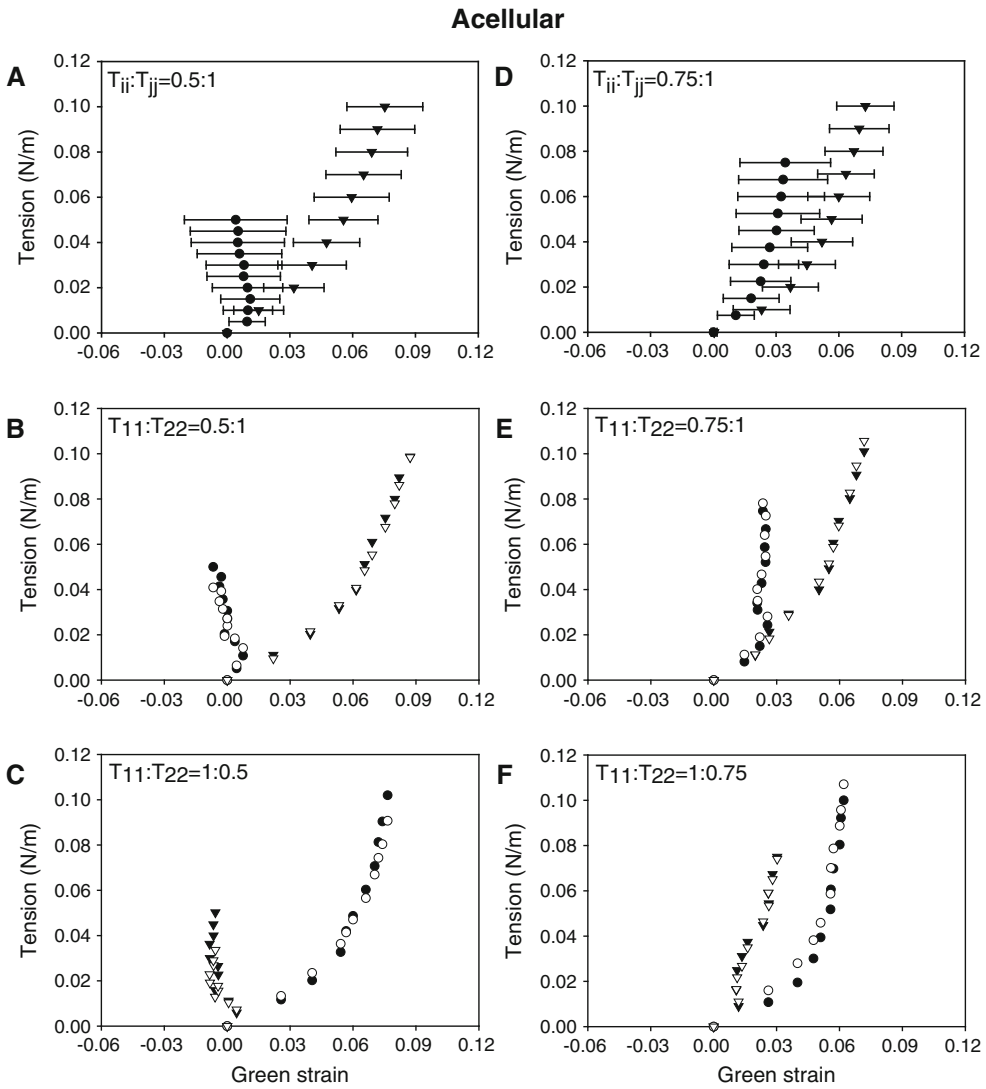

Fig. 8 Proportional tension data for acellular gels (**a** T_{ii}:T_{jj} = 0.5:1, **d** T_{ii}:T_{jj} = 0.75:1; i, j are the orthogonal directions). Representative proportional tension data (*solid symbols*) from an acellular gel and the fits (*open symbols*) by the Fung model (**b** T_{11}:T_{22} = 0.5:1, **c** T_{11}:T_{22} = 1:0.5, **e** T_{11}:T_{22} = 0.75:1, **f** T_{11}:T_{22} = 1:0.75). *Filled circle* and *open circle* $T_{11} - E_{11}$, *filled inverted triangle* and *open inverted triangle* $T_{22} - E_{22}$. Note that the best-fit material parameters were used to predict the mechanical behavior of the gel under equibiaxial tension in Fig. 15

behavior. Indeed, in order to fully characterize the mechanical behavior of cell-seeded collagen gels, the biphasic characteristics of the gel and the viscoelastic properties of collagen fibers must be taken into account. Nevertheless, the purpose of mechanical testing in this study was to probe the tensile behavior of the solid network phase of the gel as our focus is on the remodeling of the solid network phase due to the various mechanical constraints.

In this study, sequential measurements of mechanical properties were performed on each gel before and after decellularization. Cell traction is believed to participate in reversible collagen fiber alignment. Removal of cells or deactivation of cell traction thus reveals the passive mechanical properties that may have been irreversibly changed. Generally, irreversible collagen fiber alignment involves mechanisms such as formation of chemical bonds that entrench alignment or matrix deposition at preferred orientations. Marenzana et al. (2006) used a transducer to monitor directly the forces generated by fibroblast-populated collagen gels over 60 h of culture and showed that tension results from a combination of cell-mediated traction and a gradually increasing "residual matrix tension." They suggested that this residual matrix tension, which accounted for ~50 % of measured force after 60 h of culture, indicated "a time-dependent shortening of the collagen network, progressively stabilized into a built-in tension within the matrix." The irreversible mechanical anisotropy found in this study is consistent with the existence of a residual matrix tension that is presum-

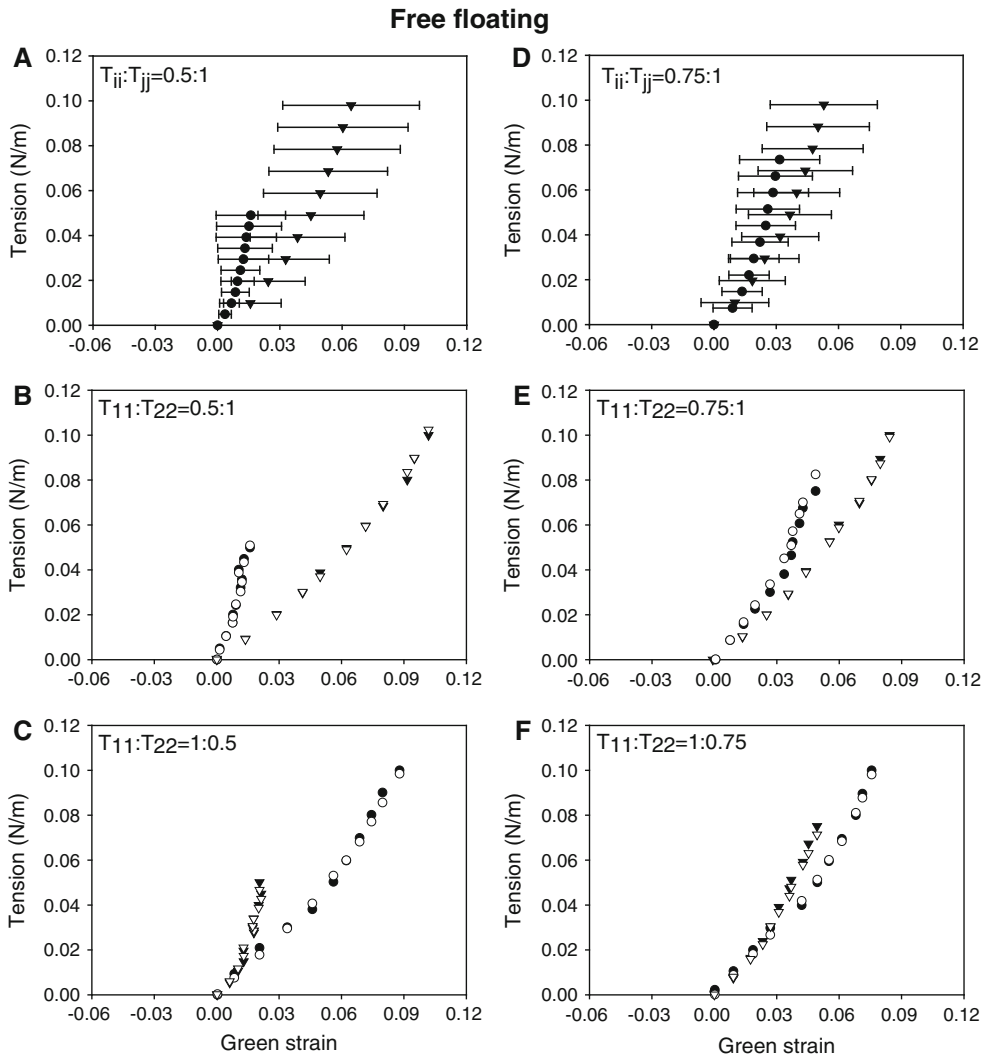

Fig. 9 Proportional tension data for decellularized gels that were cultured under the free-floating condition (**a** T_{ii}:T_{jj} = 0.5:1, **d** T_{ii}:T_{jj} = 0.75:1; i, j are the orthogonal directions). Representative proportional tension data (*solid symbols*) from a gel of the group and the fits (*open symbols*) by the Fung model (**b** T_{11}:T_{22} = 0.5:1, **c** T_{11}:T_{22} = 1:0.5, **e** T_{11}:T_{22} = 0.75:1, **f** T_{11}:T_{22} = 1:0.75). *Filled circle* and *open circle* $T_{11} - E_{11}$, *filled inverted triangle* and *open inverted triangle* $T_{22} - E_{22}$. Note that the best-fit material parameters were used to predict the mechanical behavior of the gel under equibiaxial tension in Fig. 15

ably related to a tendency toward tensional homeostasis. A similar "stable remodeling" of collagen gels by fibroblasts was reported by Sawhney and Howard (2002), who emphasized the importance of fibroblast-generated traction fields in remodeling the matrix as reemphasized by Dahlmann-Noor et al. (2007).

The mechanical properties of gels cultured under the free-floating condition had a greater variability than the other gels that were cultured under the mechanical constraints. In the free-floating condition, the porous bars at the end of the arms of the gel were actually floated over the medium while the gel was suspended in the medium. Although efforts were made to make the gel and porous bars at the same level, the shape of the gel after 6 days of culture generally deviated from the original cruciform shape. This may lead to a regionally heterogeneous microstructure and result in the great variation in the mechanical properties.

Two methods of attaching a specimen to a loading system have proven particularly useful in biaxial mechanical testing of planar soft tissues: the use of arrays of sutures to couple square specimens to the system and the use of end-clamps to couple cruciform specimens to the system (Humphrey et al. 2008). Although neither experimental configuration is perfect, the limited suture retention strength of collagen gels suggests the use of cruciform samples wherein ends can be secured well for loading. Waldman and Lee (2005) showed in native pericardium, for example, that mechanical properties can be estimated consistently using cruciform-shaped

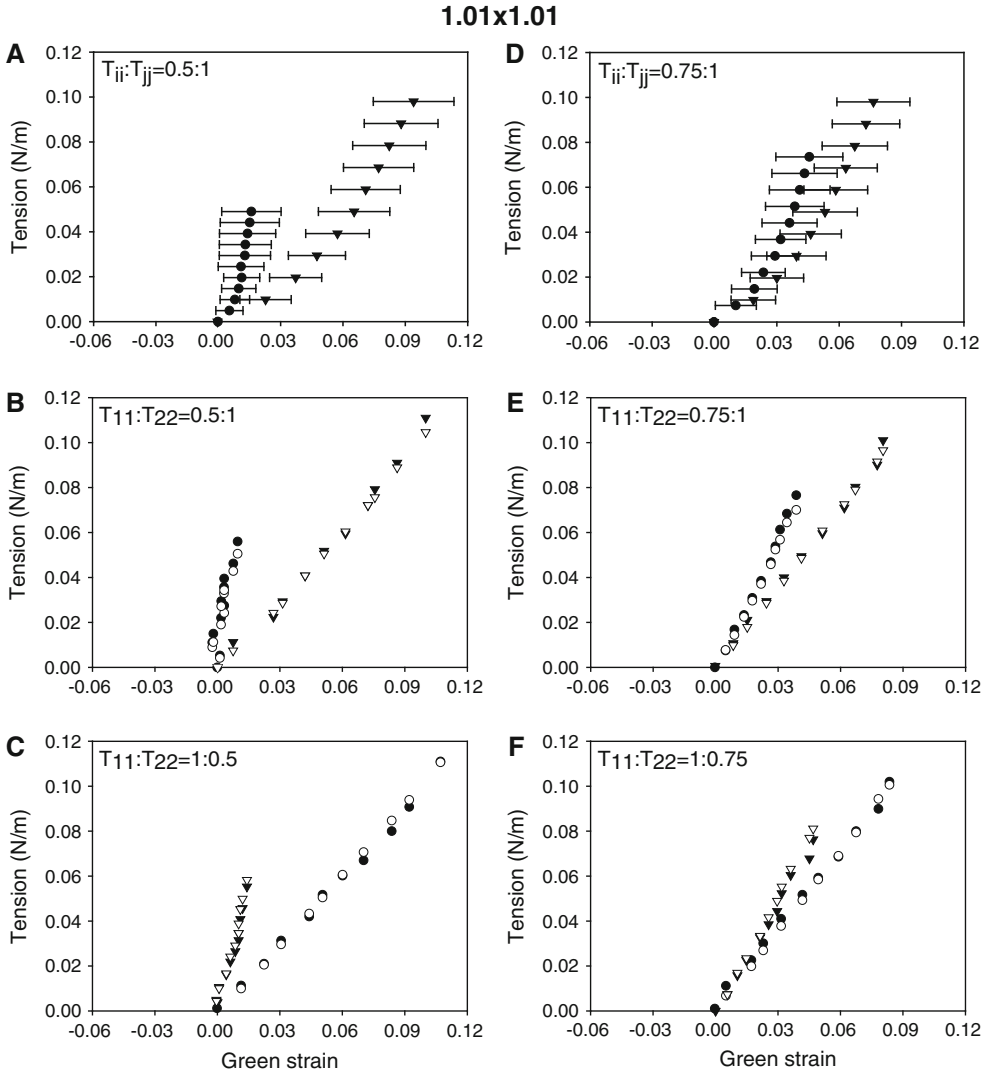

Fig. 10 Proportional tension data for decellularized gels that were cultured under the 1.01×1.01 equibiaxial stretching condition (**a** T_{ii}:T_{jj} = 0.5:1, **d** T_{ii}:T_{jj} = 0.75:1; i, j are the orthogonal directions). Representative proportional tension data (*solid symbols*) from a gel of the group and the fits (*open symbols*) by the Fung model (**b** T_{11}:T_{22} = 0.5:1, **c** T_{11}:T_{22} = 1:0.5, **e** T_{11}:T_{22} = 0.75:1, **f** T_{11}:T_{22} = 1:0.75). *Filled circle* and *open circle* $T_{11} - E_{11}$, *filled inverted triangle* $T_{22} - E_{22}$. Note that the best-fit material parameters were used to predict the mechanical behavior of the gel under equibiaxial tension in Fig. 15

samples wherein the arms are 50–100 % of the length of the central region, but samples with arms only 5 % of the length of the central region result in an overly constrained material with an artificially high stiffness. Whereas Thomopoulos et al. (2005) used biaxial specimens with very short arms, our cruciform specimens had arms 200 % of the length of the central region. Also note that Waldman and Lee (2005) cautioned that "any non-symmetrical fiber arrangement about the material test axes should produce a centralized sample rotation toward the direction of stretch under equibiaxial loading." For all of the gels examined in this study, both the shear strain and the rigid body rotation angle in the central region were negligible throughout the test, suggesting that the collagen fibers in the central region were either randomly oriented or symmetrically aligned to one of the material test axes. This, in fact, is consistent with microstructural findings reported in the previous study (Hu et al. 2009). Note that it is important not to infer shear information from planar biaxial tests because of the inability to impose defined shear stresses (Holzapfel and Ogden 2009).

In this study, the cell seeding density was twice as much as that used in the previous study. Perhaps limited by the sensitivity of the force transducer, our preliminary experiments showed that mechanical properties of the gel were not significantly changed at day 3 or if the original (i.e., half of the current study) cell seeding density was used. These

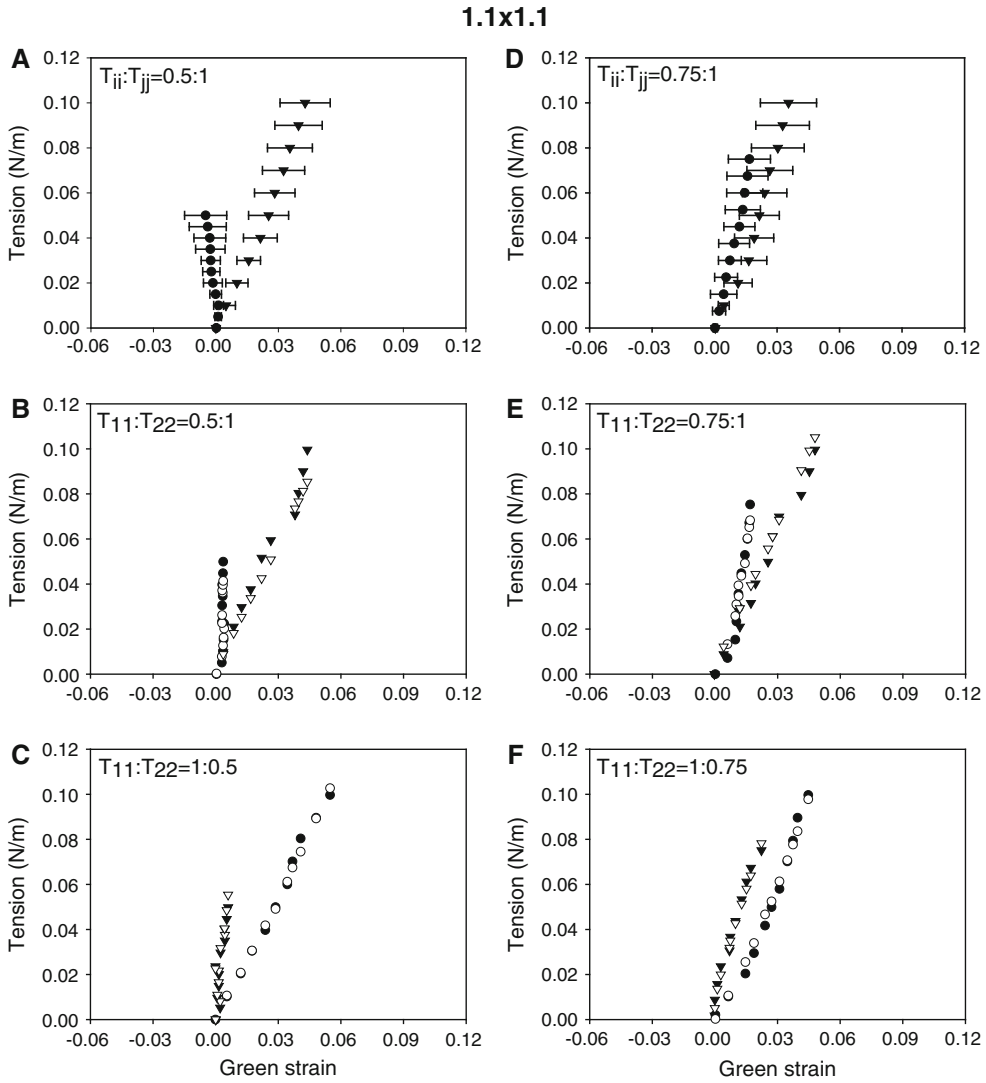

Fig. 11 Proportional tension data for decellularized gels that were cultured under the 1.1 × 1.1 equibiaxial stretching condition (**a** T_{ii}:T_{jj} = 0.5:1, **d** T_{ii}:T_{jj} = 0.75:1; i, j are the orthogonal directions). Representative proportional tension data (*solid symbols*) from a gel of the group and the fits (*open symbols*) by the Fung model (**b** T_{11}:T_{22} = 0.5:1, **c** T_{11}:T_{22} = 1:0.5, **e** T_{11}:T_{22} = 0.75:1, **f** T_{11}:T_{22} = 1:0.75). *Filled circle* and *open circle* $T_{11} - E_{11}$, *filled inverted triangle* and *open inverted triangle* $T_{22} - E_{22}$. Note that the best-fit material parameters were used to predict the mechanical behavior of the gel under equibiaxial tension in Fig. 15

indicated the important role of cells and culturing time in the remodeling of the gels. Note that although the sensitivity of the force transducer can be further increased, it may complicate the mechanical testing as the determination of the unloaded, reference state of the gel, which is the most technically difficult part in this study, could become more challenging.

It was found that planar biaxial constraints, in contrast to the uniaxial constraint, prohibit development of an extreme structural anisotropy due to gel compaction and that structural anisotropy imposed initially in a strip-biaxially stretched region of a gel became irreversible after 6 days of culture (Hu et al. 2009). It is interesting to note that the structural anisotropy was not obvious until embedded cells were removed; that is, cell traction appeared to interfere in the observation of irreversible fiber re-orientation. The mechanical anisotropy developed by the strip-biaxial stretching became less obvious after decellularization, however, suggesting that the embedded cells by themselves may be positively involved in the mechanical anisotropy and cell traction may not influence the mechanical anisotropy of the gel. Also note that 6 days may not be sufficient to obtain consistent, fully irreversible mechanical anisotropy for the gels. As the biaxial mechanical properties of the gels were examined at day 6 only, it remains to be clarified whether the mechanical anisotropy induced by

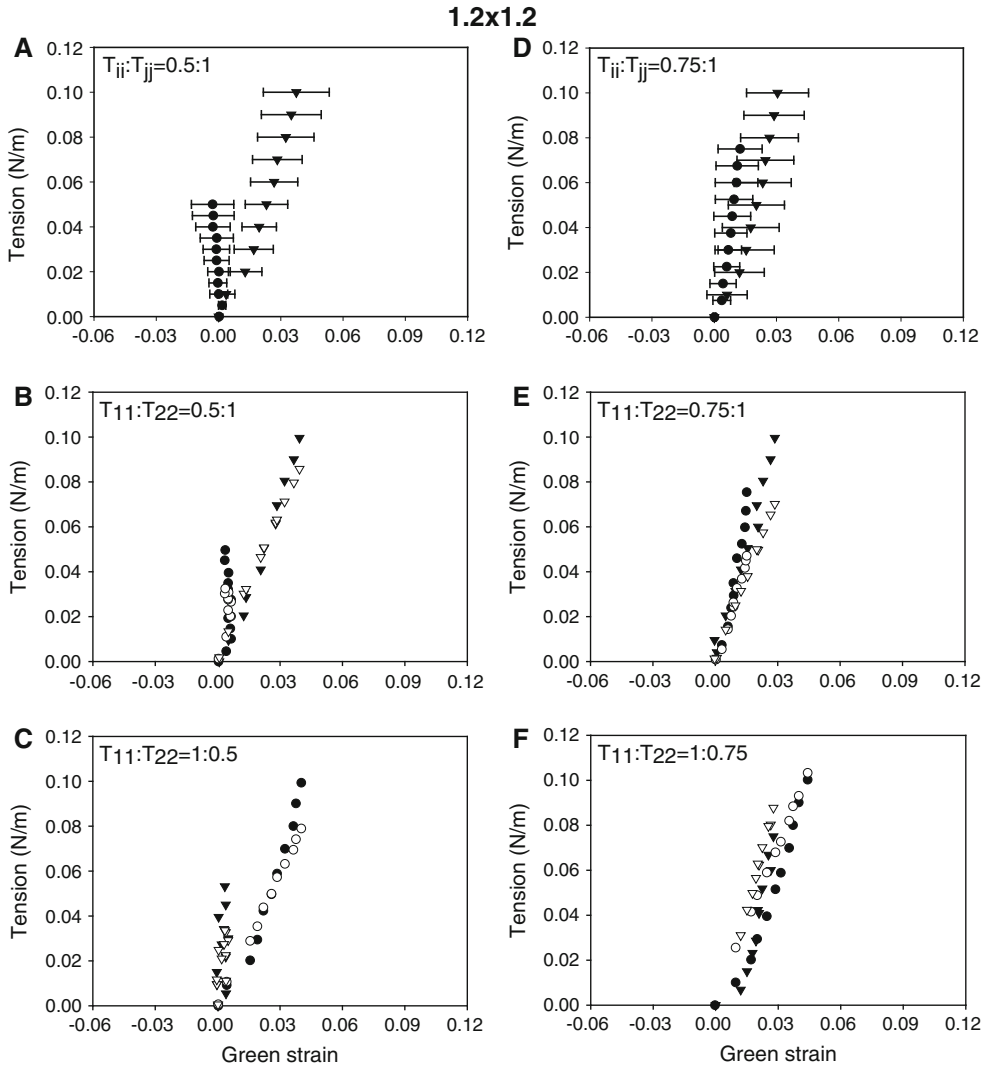

Fig. 12 Proportional tension data for decellularized gels that were cultured under the 1.2 × 1.2 equibiaxial stretching condition (**a** T_{ii}:T_{jj} = 0.5:1, **d** T_{ii}:T_{jj} = 0.75:1; i, j are the orthogonal directions). Representative proportional tension data (*solid symbols*) from a gel of the group and the fits (*open symbols*) by the Fung model (**b** T_{11}:T_{22} = 0.5:1, **c** T_{11}:T_{22} = 1:0.5, **e** T_{11}:T_{22} = 0.75:1, **f** T_{11}:T_{22} = 1:0.75). *Filled circle* and *open circle* $T_{11} - E_{11}$, *filled inverted triangle* and *open inverted triangle* $T_{22} - E_{22}$. Note that the best-fit material parameters were used to predict the mechanical behavior of the gel under equibiaxial tension in Fig. 15

culturing under the strip-biaxial stretching condition will be enhanced or remain unchanged beyond 6 days of culture. Note also that cell-seeded collagen gels, like other native or artificial tissues that contain cells, are capable of remodeling themselves to adapt environments. Lee et al. (2008) demonstrated that anisotropic cell-seeded collagen gels that are initially developed under mechanical constraints undergo structural and mechanical remodeling in response to altered loading conditions. As pointed out by Lee et al., it needs to be emphasized that cell-seeded tissue substitutes can undergo growth and remodeling and their structural and mechanical properties may change over time after implantation.

Although the Fung model appeared to fit the nonlinear tension-strain curves well, it did not perform comparably well on the linear tension-strain curves probably due to the nature of the exponential function in the model. Nevertheless, quantification of the biaxial mechanical properties by the model provided valuable indices for statistical comparisons. Note also that if the data of each gel in the same group were combined for fitting, the r^2 of all of the groups were poor. Although it may in part be explained by the variations in the mechanical behavior of the gels, it could be attributed to the use of an inappropriate model. Finally, the Fung model is purely phenomenological, involves no structural information, and has limited physical meaning. Structure-motivated

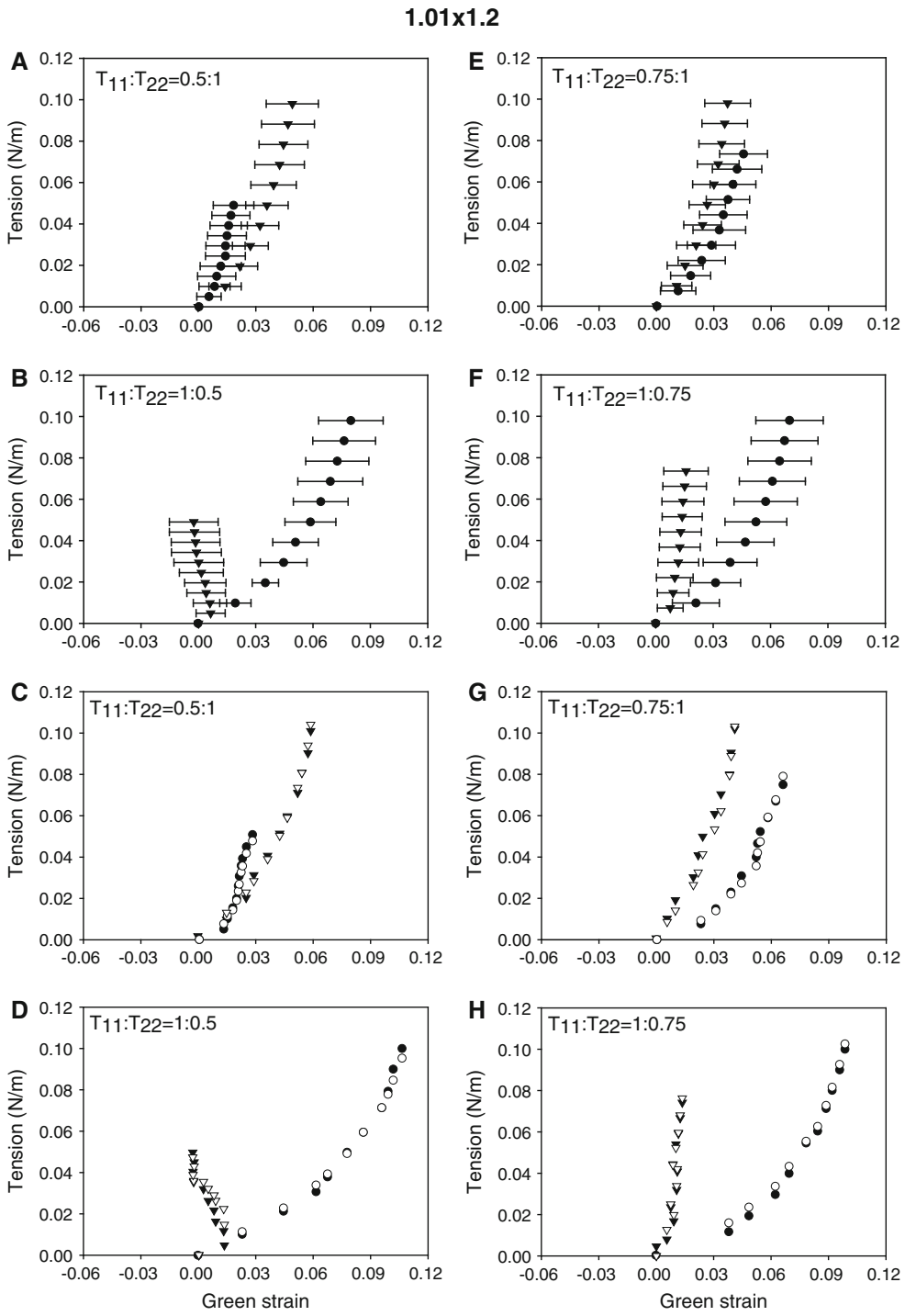

Fig. 13 Proportional tension data for decellularized gels that were cultured under 1.01 × 1.2 strip-biaxial stretching condition (**a** T_{11}:T_{22} = 0.5:1, **b** T_{11}:T_{22} = 1:0.5, **e** T_{11}:T_{22} = 0.75:1, **f** T_{11}:T_{22} = 1:0.75). Representative proportional tension data (*solid symbols*) from a gel of the group and the fits (*open symbols*) by the Fung model (**c** T_{11}:T_{22} = 0.5:1, **d** T_{11}:T_{22} = 1:0.5, **g** T_{11}:T_{22} = 0.75:1, **h** T_{11}:T_{22} = 1:0.75). *Filled circle* and *open circle* $T_{11} - E_{11}$, *filled inverted triangle* and *open inverted triangle* $T_{22} - E_{22}$. Note that the best-fit material parameters were used to predict the mechanical behavior of the gel under equibiaxial tension in Fig. 15

phenomenological constitutive models (e.g., Lanir 1983; Humphrey and Yin 1987) that may help elucidate the underlying cause of mechanical behavior will be evaluated in fitting the experimental data in a future study.

Considering extraction of information from the data, it would be ideal to have a single growth and remodeling model that accounts for the outcomes of the various mechanical constraints. Development of such a model could provide more

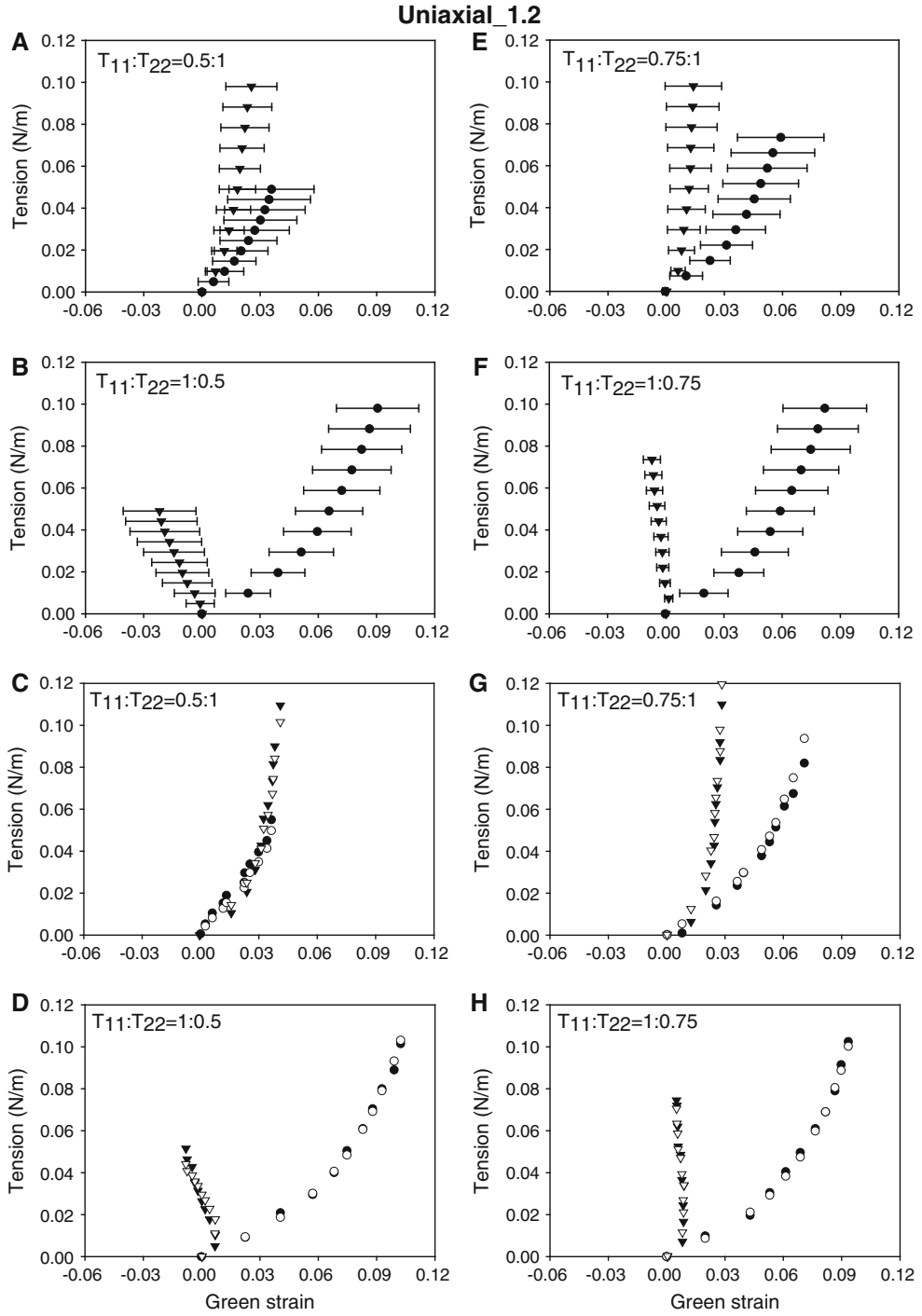

Fig. 14 Proportional tension data for decellularized gels that were cultured under 1.2 uniaxial stretching condition (**a** T_{11}:T_{22} = 0.5:1, **b** T_{11}:T_{22} = 1:0.5, **e** T_{11}:T_{22} = 0.75:1, **f** T_{11}:T_{22} = 1:0.75). Representative proportional tension data (*solid symbols*) from a gel of the group and the fits (*open symbols*) by the Fung model (**c** T_{11}:T_{22} = 0.5:1, **d** T_{11}:T_{22} = 1:0.5, **g** T_{11}:T_{22} = 0.75:1, **h** T_{11}:T_{22} = 1:0.75). *Filled circle* and *open circle* $T_{11} - E_{11}$, *filled inverted triangle* and *open inverted triangle* $T_{22} - E_{22}$. Note that the best-fit material parameters were used to predict the mechanical behavior of the gel under equibiaxial tension in Fig. 15

insight into the underlying mechanobiology. Nevertheless, additional experiments are definitely required to achieve the goal. For example, time courses of the structural and mechanical changes of gels need to be examined. Also, an aforementioned structure-based model would be more appropriate serving as a base for such a model.

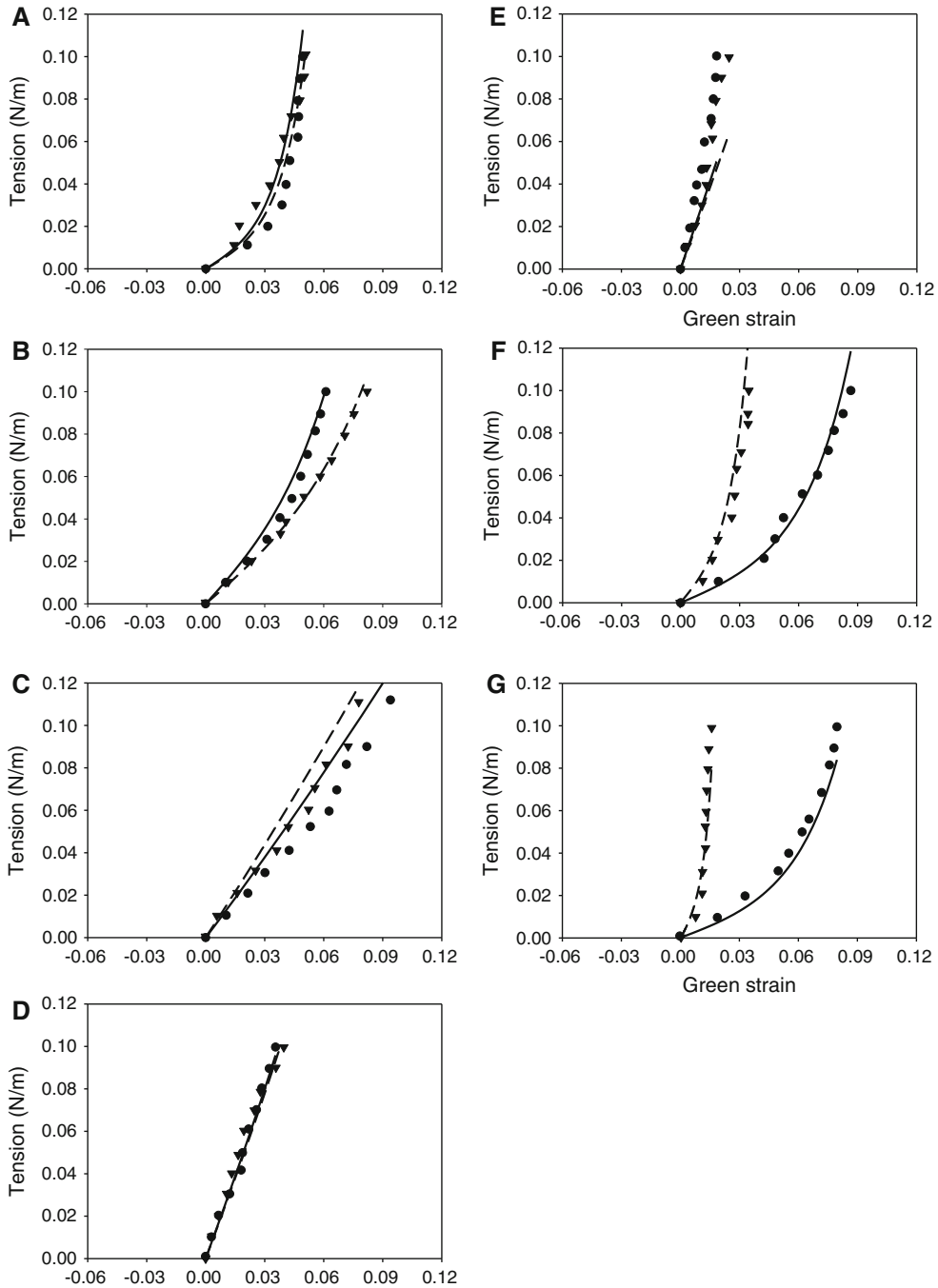

Fig. 15 Prediction of equibiaxial tension data for a representative acellular gel **a** and representative decellularized gels that were cultured under the various mechanical constraints (**b** free-floating, **c** 1.01×1.01, **d** 1.1×1.1, **e** 1.2×1.2, **f** 1.01×1.2, **g** Uniaxial_1.2). *Filled circle* (experimental data) and *solid line* (predicted values) $T_{11} - E_{11}$, *filled inverted triangle* (experimental data) and *dash line* (predicted values) $T_{22} - E_{22}$

The application of the static mechanical constraints in this study represents a single mechanical stimulus; its effects may decay over time. Cyclic stretching, on the other hand, represents a continuous mechanical stimulus. In fact, most cells in the body are under dynamic mechanical stimuli in physiological conditions. We have thus designed and built a planar biaxial dynamic stretcher, onto which our culturing chamber can be mounted. The influence of cyclic biaxial stretching on these gels will be examined, which likely will lead to better understanding of the role of mechanical conditioning on tissue development.

5 Conclusions

This study demonstrated that the various mechanical constraints have different effects on the biaxial mechanical properties of the cell-seeded collagen gels. The nonlinear pseudo-elastic properties of the gels were quantified by the Fung model. Statistical comparisons of stiffness and mechanical anisotropy for the various mechanical constraints were made. Culturing under the strip-biaxial stretching condition resulted in the gels with a modest degree of mechanical anisotropy while the uniaxial stretching induced a strong degree of mechanical anisotropy in the gels. Although the gels cultured under the equibiaxial stretching condition remained mechanically isotropic, increased extent of equibiaxial stretching increased the stiffness of the gel significantly.

Acknowledgments This research was supported by a grant from the National Science Council in Taiwan (NSC-97-2218-E-006-289-MY2).

References

Bell E, Ivarsson B, Merrill C (1979) Production of a tissue-like structure by contraction of collagen lattices by human-fibroblasts of different proliferative potential invitro. Proc Natl Acad Sci USA 76(3): 1274–1278

Berry CC, Shelton JC, Lee DA (2009) Cell-generated forces influence the viability, metabolism and mechanical properties of fibroblast-seeded collagen get constructs. J Tissue Eng Regen Med 3(1): 43–53

Brown RA, Wiseman M, Chuo CB, Cheema U, Nazhat SN (2005) Ultrarapid engineering of biomimetic materials and tissues: Fabrication of nano- and microstructures by plastic compression. Adv Funct Mater 15(11): 1762–1770

Chandran PL, Barocas VH (2004) Microstructural mechanics of collagen gels in confined compression: Poroelasticity, viscoelasticity, and collapse. J Biomech Eng Trans ASME 126(2): 152–166

Chen MY, Sun YL, Zhao C, Zobitz ME, An KN, Moran SL, Amadio PC (2008) Substrate adhesion affects contraction and mechanical properties of fibroblast populated collagen lattices. J Biomed Mater Res Part B Appl Biomater 84B(1): 218–223

Dahlmann-Noor AH, Martin-Martin B, Eastwood M, Khaw PT, Bailly M (2007) Dynamic protrusive cell behaviour generates force and drives early matrix contraction by fibroblasts. Exp Cell Res 313(20): 4158–4169

Ehrlich HP (1988) Wound closure—evidence of cooperation between fibroblasts and collagen matrix. Eye 2: 149–157

Feng Z, Tateishi Y, Nomura Y, Kitajima T, Nakamura T (2006) Construction of fibroblast-collagen gels with orientated fibrils induced by static or dynamic stress: toward the fabrication of small tendon grafts. J Artif Organs 9(4): 220–225

Grenier G, Remy-Zolghadri M, Larouche D, Gauvin R, Baker K, Bergeron F, Dupuis D, Langelier E, Rancourt D, Auger FA, Germain L (2005) Tissue reorganization in response to mechanical load increases functionality. Tissue Eng 11(1–2): 90–100

Grodzinsky AJ, Levenston ME, Jin M, Frank EH (2000) Cartilage tissue remodeling in response to mechanical forces. Annu Rev Biomed Eng 2:691–713

Harris AK, Stopak D, Wild P (1981) Fibroblast traction as a mechanism for collagen morphogenesis. Nature 290(5803): 249–251

Holzapfel GA, Gasser TC, Ogden RW (2000) A new constitutive framework for arterial wall mechanics and a comparative study of material models. J Elast 61(1–3): 1–48

Holzapfel GA, Ogden RW (2009) On planar biaxial tests for anisotropic nonlinearly elastic solids. A continuum mechanical framework. Math Mech Solids 14(5): 474–489

Hu JJ, Fossum TW, Miller MW, Xu H, Liu JC, Humphrey JD (2007) Biomechanics of the porcine basilar artery in hypertension. Ann Biomed Eng 35(1): 19–29

Hu JJ, Humphrey JD, Yeh AT (2009) Characterization of engineered tissue development under biaxial stretch using nonlinear optical microscopy. Tissue Eng Part A 15(7): 1553–1564

Humphrey JD (1999) An evaluation of pseudoelastic descriptors used in arterial mechanics. J Biomech Eng Trans ASME 121(2): 259–262

Humphrey JD, Strumpf RK, Yin FCP (1992) A constitutive theory for biomembranes—application to epicardial mechanics. J Biomech Eng Trans ASME 114(4): 461–466

Humphrey JD, Wells PB, Baek S, Hu JJ, McLeroy K, Yeh AT (2008) A theoretically-motivated biaxial tissue culture system with intravital microscopy. Biomech Model Mechanobiol 7(4): 323–334

Humphrey JD, Yin FCP (1987) A new constitutive formulation for characterizing the mechanical-behavior of soft-tissues. Biophys J 52(4): 563–570

Kjaer M (2004) Role of extracellular matrix in adaptation of tendon and skeletal muscle to mechanical loading. Physiol Rev 84(2): 649–698

Knezevic V, Sim AJ, Borg TK, Holmes JW (2002) Isotonic biaxial loading of fibroblast-populated collagen gels: a versatile, low-cost system for the study of mechanobiology. Biomech Model Mechanobiol 1(1): 59–67

Langdon SE, Chernecky R, Pereira CA, Abdulla D, Lee JM (1999) Biaxial mechanical/structural effects of equibiaxial strain during crosslinking of bovine pericardial xenograft materials. Biomaterials 20(2): 137–153

Lanir Y (1983) Constitutive equations for fibrous connective tissues. J Biomech 16(1): 1–12

Lee EJ, Holmes JW, Costa KD (2008) Remodeling of engineered tissue anisotropy in response to altered loading conditions. Ann Biomed Eng 36(8): 1322–1334

Lincoln J, Lange AW, Yutzey KE (2006) Hearts and bones: shared regulatory mechanisms in heart valve, cartilage, tendon, and bone development. Dev Biol 294(2): 292–302

Marenzana M, Wilson-Jones N, Mudera V, Brown RA (2006) The origins and regulation of tissue tension: identification of collagen tension-fixation process in vitro. Exp Cell Res 312(4): 423–433

Mauck RL, Soltz MA, Wang CCB, Wong DD, Chao PHG, Valhmu WB, Hung CT, Ateshian GA (2000) Functional tissue engineering of articular cartilage through dynamic loading of chondrocyte-seeded agarose gels. J Biomech Eng Trans ASME 122(3): 252–260

Mcculloch AD, Smaill BH, Hunter PJ (1987) Left-ventricular epicardial deformation in isolated arrested dog heart. Am J Physiol Heart Circ Physiol 252(1): H233–H241

Mol A, Driessen NJB, Rutten MCM, Hoerstrup SP, Bouten CVC, Baaijens FPT (2005) Tissue engineering of human heart valve leaflets: A novel bioreactor for a strain-based conditioning approach. Ann Biomed Eng 33(12): 1778–1788

Sawhney RK, Howard J (2002) Slow local movements of collagen fibers by fibroblasts drive the rapid global self-organization of collagen gels. J Cell Biol 157(6): 1083–1091

Seliktar D, Black RA, Vito RP, Nerem RM (2000) Dynamic mechanical conditioning of collagen-gel blood vessel constructs induces remodeling in vitro. Ann Biomed Eng 28(4): 351–362

Shearn JT, Juncosa-Melvin N, Boivin GP, Galloway MT, Goodwin W, Gooch C, Dunn MG, Butler DL (2007) Mechanical stimulation of tendon tissue engineered constructs: Effects on construct stiffness,

repair biomechanics, and their correlation. J Biomech Eng Trans ASME 129(6): 848–854
Shi YL, Vesely I (2003) Fabrication of mitral valve chordae by directed collagen gel shrinkage. Tissue Eng 9(6): 1233–1242
Thomopoulos S, Fomovsky GM, Holmes JW (2005) The development of structural and mechanical anisotropy in fibroblast populated collagen gels. J Biomech Eng Trans ASME 127(5): 742–750
Wagenseil JE, Mecham RP (2009) Vascular extracellular matrix and arterial mechanics. Physiol Rev 89(3): 957–989
Waldman SD, Lee JM (2005) Effect of sample geometry on the apparent biaxial mechanical behaviour of planar connective tissues. Biomaterials 26(35): 7504–7513
Wells PB, Yeh AT, Humphrey JD (2006) Influence of glycerol on the mechanical reversibility and thermal damage susceptibility of collagenous tissues. IEEE Trans Biomed Eng 53(4): 747–753